

# Influence of different salts on micro-sized polyelectrolyte hollow capsules

Radostina Georgieva,\* Rumiana Dimova, Gleb Sukhorukov, Gemma Ibarz† and Helmuth Möhwald

Received 3rd June 2005, Accepted 8th July 2005

First published as an Advance Article on the web 16th August 2005

DOI: 10.1039/b507848b

Polyelectrolyte capsules of poly(styrene sulfonate, sodium salt) and poly(allylamine hydrochloride) prepared on weakly polymerized melamine formaldehyde colloidal particles have been incubated in solutions of different salts (carbonates, phosphates, chlorides). The salt concentration was varied from 0.05 to a maximum of 1.7 M. The effect of the salts on capsule topology was studied by confocal laser scanning microscopy and atomic force microscopy. The salt mediated change of permeability of the capsules was studied by fluorescence recovery after photo-bleaching. Significant size reduction with a simultaneous increase in wall thickness was found for all salt incubated samples to different extents. The changes were completed during a few minutes and were irreversible. Clear pH dependency could not be confirmed. The most remarkable effect on size, wall thickness and permeability of the capsules was found after incubation in solutions of carbonate salts. The diameter of the capsules was reduced by 20 to 25%, the thickness of the capsule walls increased by 100 to 400% and the capsules became almost impermeable for FITC labeled dextran of low molecular weight and fluorescein. Additionally, a reverse of the surface charge from positive to negative was measured for all samples treated with carbonates. A partial dissolution of the uppermost layer of poly(allylamine hydrochloride) was detected by fluorescent labeling. Layers placed deeper in the polymer film were not desorbed by the carbonate treatment. Isothermal titration calorimetric measurements showed a strong interaction of the carbonate ions with poly(allylamine hydrochloride). Carboxylation of amino groups of poly(allylamine hydrochloride) can not be excluded. The stability of the capsules at high pH values was discussed with respect to the melamine content in the multilayer. A mechanism of shrinkage due to dehydration of poly(allylamine hydrochloride) and disruption of the ion hydration shell, electrostatic screening, coiling and reorganisation of the polyelectrolytes in the multilayer was concluded.

## Introduction

The layer-by-layer (LbL) preparation of polymer films has gained increasing interest in the last ten years as a simple technique for fabricating materials with well defined and tailored chemical and physical properties.<sup>1–3</sup> The method is based on the consecutive adsorption of oppositely charged polyelectrolytes on a charged substrate.

Initially applied to planar surfaces, the approach of stepwise assembling has been extended to colloidal particles.<sup>4,5</sup> Furthermore, degradable or dissolvable colloidal particles and cells have been used as templates for multilayer assembly.<sup>6–8</sup> After film formation and core dissolution one obtains three-dimensional closed free standing films with the shape and size of the template, *i.e.*, hollow capsules made of polyelectrolytes.

Both, the coated colloids and the hollow polyelectrolyte capsules are expected to find diverse applications such as encapsulation of pharmaceuticals and bioactive molecules for specific transport, time resolved and directed release,

protection from the immune defence of the organism, biosensors for diagnosis, *etc.*<sup>9–12</sup> With respect to this broad field of application it is highly important to study the mechanisms of film formation and the factors of the environment which can influence the structure, properties and integrity of the multilayer.

Besides by electrostatic attraction the multilayer assembly is driven by entropy increase caused by the release of counter ions from the charged groups of the polyelectrolytes.<sup>5</sup> Thus the layer formation has been expected to be highly sensitive to the concentration, charge and hydration enthalpy of the salt ions in the solutions during the preparation process. In fact, it was established that the thickness of the film strongly depends on the salt concentration in the preparation medium.<sup>13–16</sup>

The post-preparative influence of salts on thickness, structure and properties of the multilayer has been less investigated until now. Studies on planar polyelectrolyte films applying neutron reflectivity<sup>17</sup> could not confirm a significant swelling of poly(allylamine hydrochloride) (PAH)/poly(styrene sulfonate, sodium salt) (PSS) films in NaCl solutions up to 2 M. Similar observations were reported by Dubas and Schlenoff where a decreasing roughness but no swelling was detected by atomic force microscopy.<sup>18</sup> These investigations concern polyelectrolyte multilayer films still attached to a substrate, which naturally could influence the structural changes induced

Max Planck Institute of Colloids and Interfaces, Am Mühlenberg 1, 14476 Golm, Germany. E-mail: radostina.georgieva@mpikg-golm.mpg.de; Fax: ++49 331 567 9202; Tel: ++49 331 9409

† Present address: University of Santiago de Compostela, Faculty of Pharmacy, Dept. Pharmaceutical Technology, 15782 Santiago de Compostela, Spain.

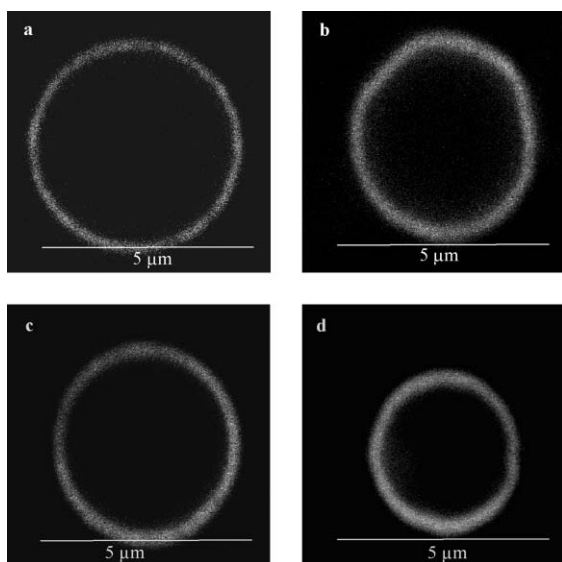


**Fig. 1** CLSM images of (PSS/PAH)<sub>4</sub> capsules in water (a) and 10 min after addition to 1.7 M solutions of CsCl (b), Na<sub>2</sub>HPO<sub>4</sub> (c) and NH<sub>4</sub>(HCO<sub>3</sub>) (d). The capsules are labelled by TRITC-PAH in the fourth layer.

by the salt. This problem can be circumvented investigating free-standing films.

As mentioned above, capsules made of polyelectrolytes by the LbL procedure represent free-standing films formed as closed shells. Changes of the permeability for macromolecules indicate some structural rearrangements in the polyelectrolyte wall of the capsules even at salt concentrations below 0.1 M.<sup>19–22</sup> Very recently, a softening effect was reported for PSS/PAH capsules in NaCl solutions with concentrations above 3 M and topological changes as a specific response to different salt species.<sup>23</sup>

In this work we investigated the response of polyelectrolyte capsules prepared on weakly polymerized melamine formaldehyde cores to solutions of different salts. The choice of salt species was made with respect to potential biological applications and included alkali chlorides, sodium phosphates and sodium carbonates. We studied changes in the size, wall thickness, permeability and  $\zeta$ -potential of the capsules applying confocal laser scanning microscopy (CLSM), atomic force microscopy, and particle electrophoresis. We also studied some

aspects of the interaction of the salt ions with the multilayer and with the polyelectrolytes in solution using isothermal titration calorimetry (ITC), fluorescence and UV/vis spectroscopy.

## Results and discussion

The topology of the capsules in aqueous solutions was studied by CLSM. First, observations were performed “online” injecting small aliquots of a capsule suspension into a drop of salt solution directly on the microscope glass. Fig. 1 shows confocal micrographs taken approximately 10 min after the capsule exposure to 1.7 M solutions of CsCl, Na<sub>2</sub>HPO<sub>4</sub> and NH<sub>4</sub>(HCO<sub>3</sub>) (Fig. 1b–d, respectively) compared with the initial state in water (Fig. 1a). It can be seen that the diameter of the capsules in water is clearly larger than the diameter of the capsules in the presence of CsCl and Na<sub>2</sub>HPO<sub>4</sub> and it decreases dramatically in the presence of NH<sub>4</sub>(HCO<sub>3</sub>). The size decrease was completed during the few minutes necessary for the capsules to sediment on the glass surface.

The capsules were further incubated in the salts listed in the methodical part at room temperature for 24 hours and studied again by CLSM. No significant further shrinkage was found. The diameter decrease was not reversible. Finally, the salt was removed by dialysis against distilled water until a conductivity of the exchanged water below 2  $\mu\text{S cm}^{-1}$  was reached. The observed size of the capsules remained the same as it was in the presence of the salts. The obtained values for the capsule diameter are presented in Table 1. It can be seen that there is no significant influence of LiCl, NaCl, Na<sub>2</sub>HPO<sub>4</sub> and NaH<sub>2</sub>PO<sub>4</sub>, a weak shrinkage of 10 and 15% in KCl and CsCl solutions, respectively, and a pronounced size reduction of more than 20% in NaHCO<sub>3</sub>, Na<sub>2</sub>CO<sub>3</sub> and NH<sub>4</sub>(HCO<sub>3</sub>).

It has to be mentioned that the capsules almost maintained their spherical shape in all investigated salts at concentrations up to 1.7 M. Some deformation was observed only if the samples had been stored in salt without stirring for longer than 24 hours. In this case the capsules form a pellet and some of them deform due to interactions with the tube walls and with the capsules in their neighbourhood. Due to the screening of the electrostatic repulsion by the salt these interactions are stronger in salt solutions, which also results in enhanced aggregation.

The conservation of the spherical shape is in discrepancy with the observations on PSS/PAH capsules prepared using

**Table 1** Diameter and wall thickness of capsules in salt solutions. The diameter of 30 to 50 capsules per sample was measured by CLSM. The AFM thickness measurements were performed on 5 capsules per sample and 10 height profiles per image

Salt solutions	$C_{\text{Salt}}/\text{M}$	pH	Diameter/ $\mu\text{m}$	Wall thickness/nm	
				estimated (see eqn (1))	measured by AFM
H <sub>2</sub> O	—	7.85	4.7 $\pm$ 0.15	12	7.3 $\pm$ 0.4
LiCl	1.67	5.95	4.6 $\pm$ 0.2	12.3	8.1 $\pm$ 0.4
NaCl	1.67	6.39	4.5 $\pm$ 0.3	13.1	10.8 $\pm$ 0.6
KCl	1.67	6.85	4.2 $\pm$ 0.4	15	11.2 $\pm$ 0.8
CsCl	1.67	6.05	4.1 $\pm$ 0.3	15.8	11.5 $\pm$ 1.1
NaH <sub>2</sub> PO <sub>4</sub>	1.67	3.92	4.5 $\pm$ 0.2	13.1	8.3 $\pm$ 0.5
Na <sub>2</sub> HPO <sub>4</sub>	1.67	8.72	4.4 $\pm$ 0.2	13.4	10.2 $\pm$ 0.8
NH <sub>4</sub> (HCO <sub>3</sub> )	1.67	8.02	3.5 $\pm$ 0.3	21.6	30.3 $\pm$ 4.3
Na <sub>2</sub> CO <sub>3</sub>	1.67	11.4	3.6 $\pm$ 0.3	20.5	15.7 $\pm$ 1.6
NaHCO <sub>3</sub>	1.3	8.56	3.7 $\pm$ 0.3	19.4	14.9 $\pm$ 1.9

polystyrene (PS) cores<sup>23,24</sup> where the addition of salt leads to pronounced buckling, caused by a transient osmotic shock. Osmotic response with the typical buckling behaviour has also been observed on MF templated capsules but only in highly concentrated solutions of polyelectrolytes, which can not permeate through the wall.<sup>25</sup> This has to be attributed to the fact that capsules prepared on MF are highly permeable for ions, small polar molecules and even for macromolecules with a molecular weight of up to 70 kDa.<sup>19</sup> Such unique behaviour of capsules assembled with the same polyelectrolytes but on different sacrificial particles can be contributed to the different dissolution procedures determined by the chemical nature of the template. The structure of the polyelectrolyte multilayer can be influenced by the different solvents, pH value and other bulk factors during the core degradation, which naturally affect its ion permeability in a very specific way. The decomposition of the weakly polymerized MF particles at low pH to oligomers leads to a high osmotic pressure in the inner volume, swelling and strong stretching of the polyelectrolyte shell,<sup>26</sup> creating relatively large defects and thus causing high permeability. In the case of PS particles an organic solvent is used to remove the core and mechanical stress does not affect the structure of the polyelectrolyte multilayer, which is reflected in much lower permeability.

However, to exclude the possibility that the capsule shrinkage is not induced by the sudden leakage of water due to an osmotic shock replacing the capsules from water to a highly concentrated salt solution, measurements with gradual increase of the salt concentration were performed. For this purpose the concentration was increased in 0.05 M steps with a delay of 10 min. Fig. 2 shows the dependence of the diameter on the salt concentration for the samples incubated with NaCl and NaHCO<sub>3</sub>. The measured diameter at the final concentration of 1.7 M for NaCl and NH<sub>4</sub>(HCO<sub>3</sub>) and 1.3 M for NaHCO<sub>3</sub> was not significantly deviating from the value obtained when these concentrations were reached in one step. It can also be seen that a significant decrease of the diameter of

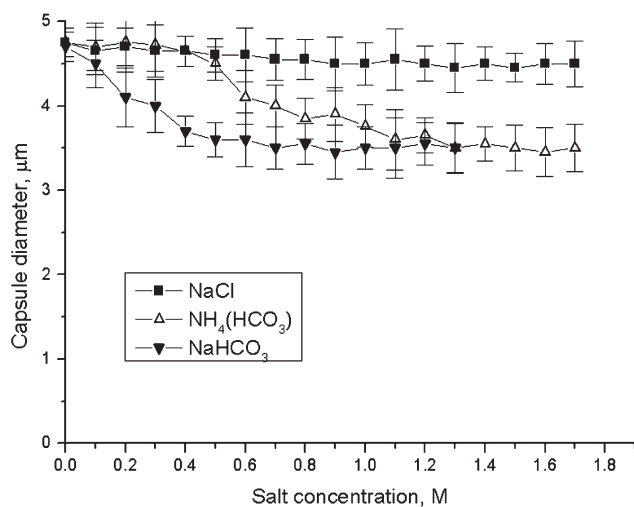


**Fig. 2** Dependence of capsule diameter on gradually increasing concentration of NaCl, NH<sub>4</sub>(HCO<sub>3</sub>) and NaHCO<sub>3</sub>. The time delay for each stepwise increase was 10 min.

the capsules in the sodium bicarbonate solution appears at a concentration of 0.2 M. For Na<sub>2</sub>CO<sub>3</sub> (curve not displayed) and NH<sub>4</sub>(HCO<sub>3</sub>) a significant size reduction was observed at concentrations above 0.6 and 1 M respectively.

It is obvious that osmotic processes are rather improbable and can not explain the dependence of the capsule size on the concentration of salts. Moreover, the diameter reduction appears to be a very slow process. The shrinkage of the capsules is completed during several minutes while osmotic response appears within seconds. Such behaviour on the longer time scale can be explained by structural changes in the multilayer introduced by the electrostatic screening of the salt ions, which weakens the bond between oppositely charged polyelectrolytes and allows conformational changes and rearrangements of the polymers in the multilayer.

If there is no dissolution of polyelectrolytes from the multilayer one can expect a constant volume of the capsule wall and the wall thickness of the shrunken capsules would increase following the relation:

$$h_S = \frac{r_0^2 \cdot h_0}{r_S^2} \quad (1)$$

where  $h_S$  is the wall thickness after salt treatment,  $h_0$  is the wall thickness of the capsules in water,  $r_0$  is the capsule radius in water and  $r_S$  is the capsule radius in salt solutions. Assuming a value of  $h_0 = 12$  nm for the thickness of the control capsules, which corresponds to the thickness of eight PAH/PSS layers as measured in water by Single Particle Light Scattering (approximately 1.5 nm per single polyelectrolyte layer),<sup>27</sup> one obtains the expected wall thickness of the capsules after salt treatment as presented in Table 1.

In parallel, the wall thickness was measured by AFM on dialysed and dried samples. Fig. 3 presents a comparison of AFM images taken from the control capsules, which were stored in water (Fig. 3a) and capsules incubated in CsCl (Fig. 3b) and NH<sub>4</sub>(HCO<sub>3</sub>) (Fig. 3c), respectively.

It is interesting that the dried surface of the carbonate samples appears wax-like and smoother than the surface of the control and of the samples treated with alkali chlorides and phosphates. The latter samples show the typical grain-like surface structure of the polyelectrolyte multilayer as observed for capsules and flat films in several studies.<sup>28,29</sup>

From Table 1 it can be seen that the thickness increases in all samples where a diameter reduction was found. The samples incubated with alkali chlorides show a tendency of size decrease and concomitant wall thickness increase corresponding to their position in the Hofmeister series. LiCl and NaCl do not affect the capsules significantly but KCl and CsCl incubation leads to size reduction of around 10% and 15%, and to a thickness increase of 50% and 60%, respectively. Carbonate salts influence the capsules much more strongly. Here, a size reduction of 20% (Na<sub>2</sub>CO<sub>3</sub> and NaHCO<sub>3</sub>) to 25% (NH<sub>4</sub>(HCO<sub>3</sub>)) was found. The wall thickness increased by a factor of 2 and 4, respectively.

Comparing the calculated and the measured values for the wall thickness (see Table 1) we found out that the measured thickness is smaller than the calculated values in eqn. (1) by about 30%. This shrinking is due to the fact that

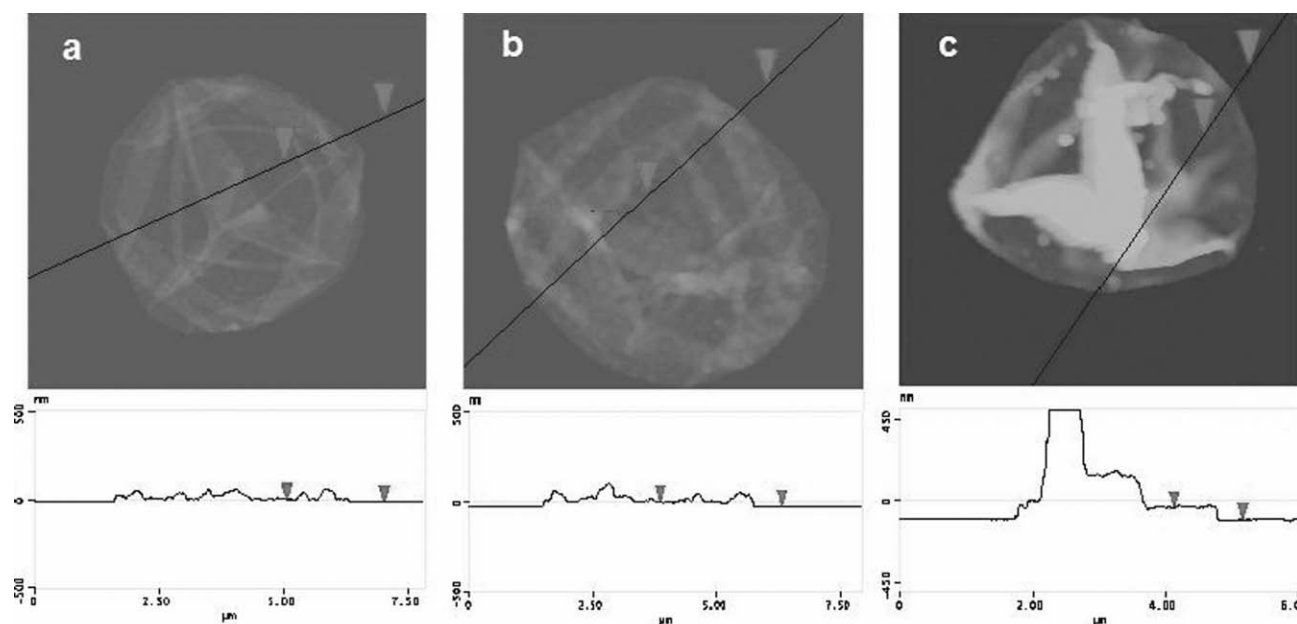


**Fig. 3** AFM images with height profiles of a) capsule in water, control; b) CsCl treated sample; c)  $\text{NH}_4(\text{HCO}_3)$  treated sample. The height scales range from  $-500$  to  $+500$  nm. The salt treatment was performed at room temperature for 24 hours followed by dialysis against water.

polyelectrolyte multilayer contains up to 50% water,<sup>30</sup> which evaporate during the drying process and lead to a reduced thickness. One exception was observed in the sample treated with ammonium bicarbonate. In this case the thickness measured by means of AFM is nearly 50% larger than the one expected theoretically for a constant film volume. It can also be seen, that the thickness increase occurs in samples which were exposed to salts with neutral or basic pH, but can be quantitatively different depending on the salt type at similar pH values, which is the case with  $\text{Na}_2\text{HPO}_4$ ,  $\text{NH}_4(\text{HCO}_3)$ , and  $\text{NaHCO}_3$ . Here, specific interactions of the ions with the polyelectrolytes have to be taken into account.

Structural rearrangements of the polyelectrolyte capsule wall under the influence of salt could also change their permeability properties. It was found by Ibarz *et al.* that PSS/PAH capsules prepared on MF cores are permeable for FITC-dextran with molecular weight up to 77000 and the permeability is sensitive to the presence of salt.<sup>19</sup> An effect of “jumping up” permeability was found in the presence of NaCl with a concentration of 0.01 M or higher. This indicates the presence of relatively large defects in the polymer film, in the range of several tens of nanometers. Since no significant size reduction was observed at such concentrations the permeability increase was attributed to electrostatic screening and enlargement of defects in the multilayer. In our experiments the permeability was measured in the absence of salt using samples where the salt was removed after 24 h incubation by dialysis. Then the control capsules and salt treated capsules were incubated with the small polar dye fluorescein and with labelled FITC-dextran. The permeation was followed by CLSM.

In the samples incubated with KCl and CsCl the permeability was measured by fluorescence recovery after photo-bleaching. The permeability of the carbonate treated capsules was too low to be measured by this technique because the

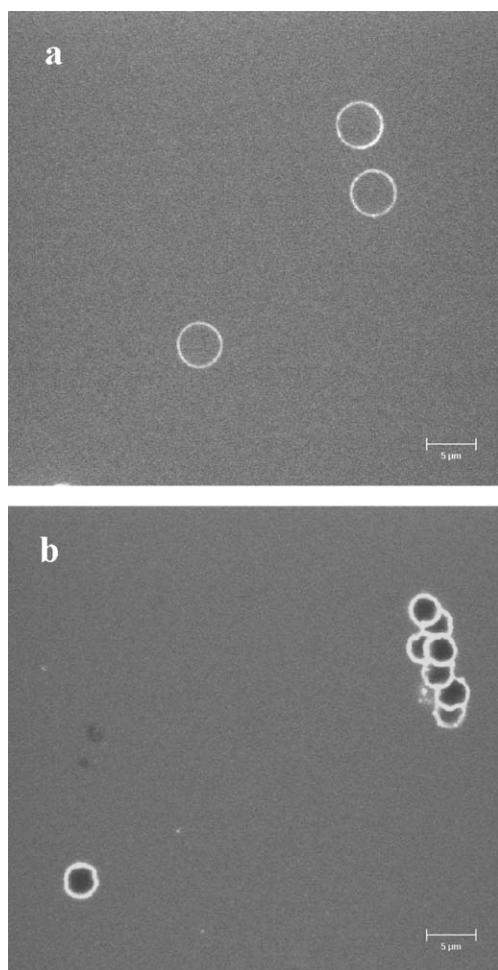
dye distribution between solution and capsule interior did not equilibrate within two hours, which makes the bleaching experiments meaningless.

Fig. 4 shows the distribution of fluorescein in the control and  $\text{NH}_4(\text{HCO}_3)$  incubated capsules before bleaching. The first micrograph shows almost equal fluorescence intensity in the environment and in the interior of the capsules. In the second picture the interior is completely dark.

Table 2 summarizes the results obtained from permeability measurements. It can be seen that the permeability for fluorescein decreases by a factor of approximately 2 after incubation with KCl and CsCl. In the case of dextran (MW 4400) only an insignificant decrease was found. Since the bleaching experiments were performed in water electrostatic repulsion could be an explanation for the observed effects if one considers uncompensated charges, resulting in defects in the multilayer. A slight shrinkage such as the one caused by alkali chlorides probably can reduce the size of the defects but cannot close them completely. For this a deeper reorganisation, such as the one probably caused by the carbonate and bicarbonate salts, is needed.

Structural changes in the polyelectrolyte multilayer could affect the charge distribution and also may influence the surface charge of the capsules, which can be shown by particle electrophoresis.

As can be seen in Fig. 5 samples incubated in alkali chlorides and phosphates keep the positive surface charge. The  $\zeta$ -potential remains between  $+45$  and  $+55$  mV. This is also the case for the sample incubated with the acidic phosphate. The basic phosphate sample shows a lower potential of around  $+30$  mV, which can be explained by a partial loss of charged groups of the upper PAH layers under the basic conditions. For the samples incubated in  $\text{Na}_2\text{CO}_3$  and  $\text{NH}_4(\text{HCO}_3)$  we obtained, in fact, negative values for the  $\zeta$ -potential of around  $-25$  mV.



**Fig. 4** CLSM micrographs, showing polyelectrolyte capsules in fluorescein solution ( $0.2 \text{ mg ml}^{-1}$ ) before (a) and after treatment with  $\text{NH}_4(\text{HCO}_3)$  (b). The observations were carried out in water. The sample treated with  $\text{NH}_4(\text{HCO}_3)$  was kept in the dye solution for 2 hours before scanning. Scale bars correspond to  $5 \mu\text{m}$ .

**Table 2** Permeability values obtained by FRAP for fluorescein and FITC-dextran (MW 4400). All measurements were performed in water

Sample	$P_{\text{fluorescein}}/\text{m s}^{-1}$	$P_{\text{dextran4400}}/\text{m s}^{-1}$
Control	$2.8 \times 10^{-7}$	$1.4 \times 10^{-7}$
KCl-incubated	$1.4 \times 10^{-7}$	$1.2 \times 10^{-7}$
CsCl-incubated	$1.2 \times 10^{-7}$	$9.2 \times 10^{-8}$
$\text{NH}_4(\text{HCO}_3)$ -incubated	too low to be measured	too low to be measured
$\text{Na}_2\text{CO}_3$ -incubated	too low to be measured	too low to be measured

The charge reversal of the carbonate treated samples could be caused by a partial or complete dissociation of the last PAH layer from the capsule surface. On the other hand, the increase of the wall thickness simultaneously with the size reduction and the restricted permeability for small polar molecules supports the idea of rearrangement processes, which take place not only on the surface. A specific interaction between the carbonate ions and PAH and possibly a chemical reaction leading to carboxylation of the amino groups of PAH can not

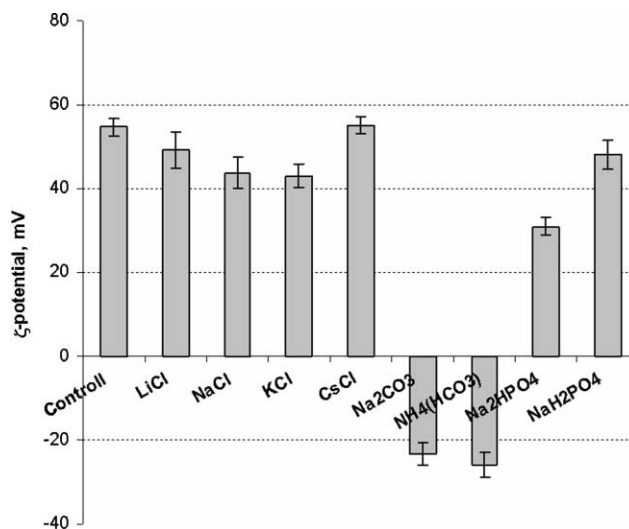


**Fig. 5** Zeta-potential of  $(\text{PSS/PAH})_4$  salt treated capsules. The treatment was performed in  $1.7 \text{ M}$  salt solutions at room temperature for 24 hours followed by dialysis against water until a conductivity of  $1$  to  $3 \mu\text{S cm}^{-1}$  was achieved. The zeta-potential measurements were performed in water.

be excluded. This would also cause a reversal of the surface charge observed by means of electrophoresis.

To detect an eventual dissolution of PAH from the capsules we labelled PAH layers placed in two different depths. In one sample the upper layer (number eight) was labelled using 10% FITC-labelled PAH and in another sample 10% TRITC-labelled PAH was applied in the sixth layer. Both samples were incubated in  $1.7 \text{ mM}$   $\text{NH}_4(\text{HCO}_3)$  for 24 hours. Afterwards the capsules were separated from the bulk by centrifugation. The absorption and fluorescence spectra of supernatants and water re-suspended pellets are shown in Fig. 6.

For the sample with FITC-labelled PAH on top the maximum absorption at  $510 \text{ nm}$  of the bicarbonate treated pellet is around 16% lower than that of the pellet of the control. In the supernatant spectrum of the same sample an absorption peak can be seen, which does not appear in the spectrum of the control supernatant (Fig. 6a). The fluorescence spectra obtained for the same sample also show a peak corresponding to FITC-PAH in the supernatant and lower fluorescence in the pellet compared to the fluorescence of the control pellet (Fig. 6b). Here the emission maximum of the supernatant of the sample is shifted towards lower wavelengths compared to that of the pellet, which typically appears if labelled substances undergo transition from an adsorbed or bound state to the state in solution. The absorption decrease of 16% corresponds to a dissociation of 16% of the layer on top. This could explain a lower surface potential but not a reversal of the sign. There is no evidence for PAH dissolution from the layers, which are placed deeper in the polyelectrolyte film. This can be seen from the absorption spectra of the  $\text{NH}_4(\text{HCO}_3)$  incubated sample with TRITC-PAH in the sixth layer (Fig. 6c). Here, the labelled substance can be detected only in the pellets but not in the supernatants for both the control and the salt treated sample. In other words, only two further polyelectrolyte layers prevent the deeper one from dissociation.

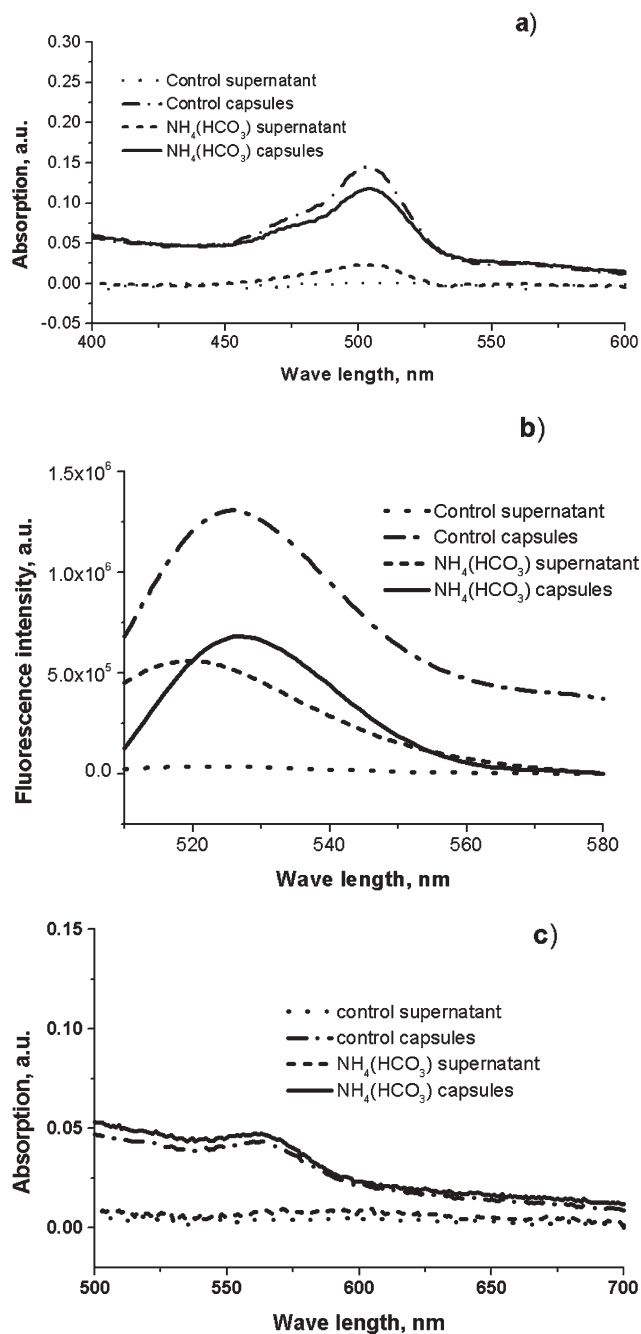


**Fig. 6** a) Absorption spectra of supernatant and pellet of capsule suspensions incubated in 1.7 M  $\text{NH}_4(\text{HCO}_3)$  solution for 24 hours. The last adsorbed layer on top of the capsules contains 10% FITC-labelled PAH. The control represents a suspension with equal capsule concentration stored in water. b) Fluorescence spectra of the samples described in a). c) Absorption spectra of supernatant and pellet of capsule suspension incubated in 1.7 M  $\text{NH}_4(\text{HCO}_3)$  solution for 24 hours. The sixth adsorbed layer contains 10% TRITC-labelled PAH.

It is well known, that polyelectrolyte complexes are sensitive to the ionic strength and the pH value of the bulk.<sup>31</sup> The behaviour depends on the excess charge of the complexes, the solubility of the individual polyelectrolytes, their charge density and the nature of their charged groups. Depending on

the salt concentration effects from flocculation to complete dissociation take place. Here we prepared measurements with stoichiometric PSS/PAH complexes in solutions of the salts applied in this study. For this purpose aqueous solutions of PAH and PSS were mixed at room temperature in equal quantities with respect to the concentration of monomers. The complexes are formed immediately after mixing, which can be seen from enhanced scattering. The salt solutions were added one hour later in order to allow stabilisation of the complexes. Then the behaviour of the complexes in the salts was studied following the changes of the optical density of the suspensions at 600 nm with time.

Fig. 7 gives the optical density (at 600 nm) as a function of time after injection of the salt solution. Since there is no absorption at this wavelength the transmission loss is due to a change in light scattering. The latter is a complex nonmonotonic function of particle size and concentration, and therefore the first 40 seconds of measurement are difficult to interpret. We therefore concentrate on the later times where the changes are due to particle dissolution. It can be seen that addition of LiCl does not influence the optical density of the complexes, which remains the same as that after addition of the same volume of water. In CsCl the behaviour is similar to that of LiCl with higher optical density. The difference was reproducible in several measurements and is probably caused by a higher density or increased size of the complexes in the presence of CsCl due to its chaotropic effect. Such behaviour would correspond well with the slight size reduction and increased wall thickness of the polyelectrolyte capsules incubated in KCl and CsCl reported above.

The effects of  $\text{NaHCO}_3$  and  $\text{Na}_2\text{CO}_3$  are more interesting. The weakly basic sodium bicarbonate dissolves the polyelectrolyte complex almost completely during a few minutes. The strong basic sodium carbonate also leads to a complete dissolution but in this case the process takes some hours. This is in discrepancy with the expected faster deprotonation of the charged amino groups of PAH at higher pH value of the bulk. One explanation could be the formation of strongly aggregated complexes, which would also explain the much higher optical

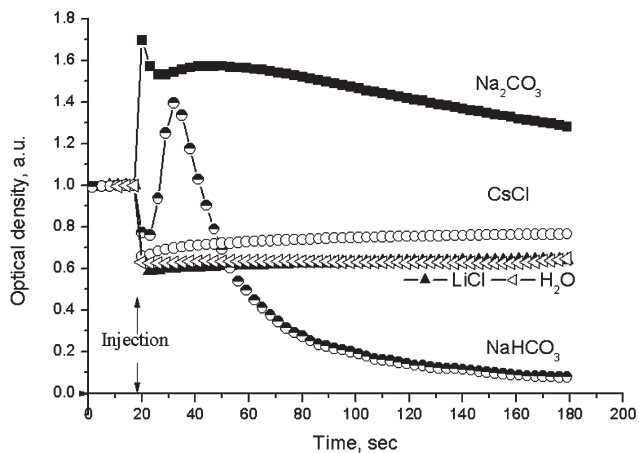


**Fig. 7** Time dependence of the optical density of PAH/PSS complexes (1 : 1 monomer concentration) at 600 nm in water and after injection of different salts (see legend). The salt concentration is 1 M.

density of the complex suspension immediately after addition of  $\text{Na}_2\text{CO}_3$  compared to that in the presence of  $\text{NaHCO}_3$ . This could reduce the accessibility of the ionic groups of PAH for the carbonate ions and obstruct the dissolution process. Nevertheless, the behaviour of the complexes correlates with the effect of the salts, which has been observed on the capsules.

The interaction of the salt solutions with polymers can be thermodynamically characterized using isothermal titration calorimetry.<sup>32–34</sup> We applied ITC to study the effects of some of the salt solutions used in this work. The interaction of each of them with PAH and PSS was probed by consecutive injections of the salt into the polymer solution. The instrument measures the heat released due to processes associated with the introduction of salt. To account for dilution effects we have performed measurements where the salt was injected in pure water. The heat of dilution was subtracted from the measurements with the polymer. The heat of dilution of the polymer solution only (injection of water in polymer solution) was negligible. The results are presented in Fig. 8 where the heat normalized by the amount of injected salt is plotted as a function of the salt concentration.

The interaction of salts with PSS (Fig. 8a) cannot be resolved because it is very close to the heat of simple dilution ( $<0.5 \text{ kJ mol}^{-1}$ ). The same was observed for the interaction between  $\text{NaCl}$  and PAH (Fig. 8b). The behaviour in the case of PAH differs drastically especially for  $\text{NaHCO}_3$ ,  $\text{NH}_4(\text{HCO}_3)$ ,  $\text{Na}_2\text{HPO}_4$ .

A very strong endothermic signal is observed with the addition of  $\text{NaHCO}_3$ , which can be associated with binding of the  $\text{HCO}_3^-$  ions to the polymer backbone. The signal decreases as the available binding sites on the polymer are exhausted. We attempted to model this process as a first order interaction corresponding to a chemical equilibrium between two species:  $\text{S} + \text{P} \leftrightarrow \text{SP}$ , where S are the free salt ions ( $\text{HCO}_3^-$ ) in the solution, P are the unoccupied ‘binding’ sites of the polymer (or free monomer units) and SP is the product, *i.e.* created bonds. The process is characterised by a molar reaction enthalpy,  $\Delta H$ , and an equilibrium constant,  $K = [\text{SP}]/([\text{S}][\text{P}])$ , where the square brackets indicate bulk concentrations. Applying the mass conservation law for the polymer and for the salt, from the equation for the equilibrium constant one can obtain an expression for [SP]. The heat released from a single titration of salt in the polymer solution would then be proportional to the molar enthalpy multiplied by the number of created bonds, *i.e.*  $\Delta H [\text{SP}]V_{\text{cell}}$ , where  $V_{\text{cell}}$  is the solution volume in the working cell. In this expression the only unknowns are  $\Delta H$  and  $K$  (which is hidden in [SP]). The latter were used as parameters to fit the data for  $\text{NaHCO}_3$  and PAH presented in Fig. 8a. From the fitting we obtain  $\Delta H = 12.5 \pm 0.4 \text{ kJ mol}^{-1}$  and  $K = 0.10 \pm 0.03 \text{ mM}^{-1}$ . We recall that the measurement shows that this interaction is an endothermic process. This implies that it is entropically driven. From  $K$  one can make an estimate of the Gibbs free energy:  $\Delta G = -RT \ln(K \times 55.5)$ . The factor 55.5, which is the concentration of water in units of  $\text{mol l}^{-1}$ , is introduced to account for the dimensionality of  $K$ . For  $\Delta G$  we obtain a value around  $-21.4 \text{ kJ mol}^{-1}$ . Then for the entropy term of the interaction we estimate  $T\Delta S = 13.6k_{\text{B}}T$ , where  $T$  is temperature and  $k_{\text{B}}$  is the Boltzmann factor. This corresponds to

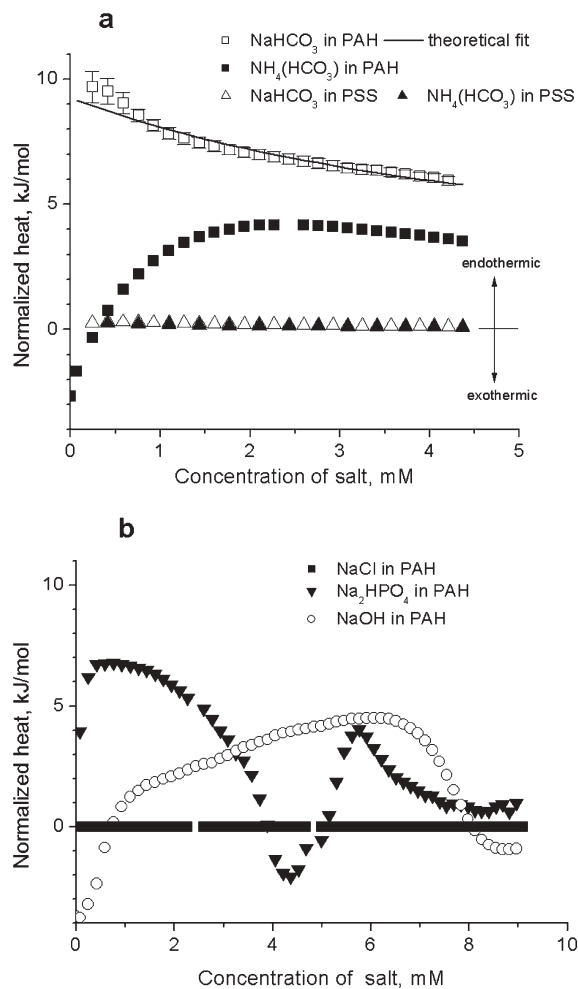


**Fig. 8** ITC measurements of the normalized heat (released heat per moles injected salt) as a function of the salt concentration. Positive value of the signal indicates an endothermic process and *vice versa* as indicated by the arrows in a). 50 mM of each salt injected in solutions of 9.3 mM PAH (monomer concentration) and 4.5 mM PSS (monomer concentration) (see legend). The heat associated with dilution of the salt in water has been subtracted. The solid line presents a theoretical fit (see text for details).

liberation of around 8 water molecules if all the energy of the process is associated with dehydration of the polymer and disruption of the ion hydration shell. Of course, apart from hydrogen bonding, one can expect also entropic contributions from conformational changes of the polymer. The theoretical modelling was applied only to this salt–polymer system because it showed monotonic behaviour. In the rest of the cases the exhibition of a maximum is characteristic for the occurrence of two (or more) competing processes as more salt is added to the system. For example, one can speculate that a chemical reaction between the  $\text{NH}_3^+$  groups of PAH and  $\text{HCO}_3^-$  or  $\text{CO}_3^{2-}$  ions takes place. These processes may be responsible also for the small deviation of measurement and fit encountered at low salt concentrations in the case of  $\text{NaHCO}_3$ . Additional complications leading to problems in the interpretation of the calorimetry data in Fig. 8b are that salt addition changes the pH and that stoichiometric complexes

may be formed and precipitate. The latter explains the minimum of the curve for  $\text{Na}_2\text{HPO}_4$  at 4.2 mM and for  $\text{NaOH}$  at 8.5 mM. Indeed, in the case of addition of  $\text{Na}_2\text{HPO}_4$  the turbidity of the solution was found to change during the measurement (see below).

In conclusion, the predominantly endothermic signal from the titration calorimetry data suggests that the interaction of all salts with PAH is strongly associated with a significant entropy change in the system. In the case of ammonium bicarbonate the titration curve above a salt concentration of 2 mM is nearly parallel to that of  $\text{NaHCO}_3$ , which suggests a similar mechanism of interaction. The initial increase of the signal can be attributed to pH changes, which are usually associated with an exothermic signal. We did not attempt to apply the model described above to the PAH titration with the other salts because the data suggest a physically different and more complex behaviour of the system (the absolute value of the signal does not decrease suggesting competing processes). We speculate that this behaviour may be associated with pH effects with coiling of the polymer due to a change of the Debye screening length as the salt is added.

Finally, we can summarize that the effect of salt on the size of PSS/PAH capsules correlates with the measured wall thickness and reduced permeability for small polar dyes. The effect is associated mainly with the interaction of the salts with the weak polycation PAH. The absence of an effect of the sodium phosphates was surprising, because a strong affinity of the phosphate anion to PAH is known. This was confirmed by the ITC measurements and a precipitation of the polymer was visible in the solution at the final concentration of titration. One explanation of the very weak influence on the capsule topology could be the very low solubility of the PAH/phosphate complex, which hinders its dissolution from the surface of the multilayer.

The reversal of the surface charge of the capsules from positive to negative under the influence of bicarbonate and carbonate salts can be ascribed to a partial dissolution of the uppermost PAH layer as was shown by fluorescently labelled PAH. This correlates with the dissolution kinetics of stoichiometric PSS/PAH complexes observed from optical density measurements. A chemical reaction, probably a carboxylation of  $\text{NH}_3^+$  groups, cannot be excluded and would explain the complete charge reversal. Such a possibility was taken into account in the explanation of the ITC curves.

Finally, we bring the attention to the significant stability of the MF templated PSS/PAH capsules. Stored in salt solutions of high concentration, apart from some aggregation and deformation, the capsules could not be decomposed during several months. This is in contradiction to the behaviour reported for PSS/PAH capsules even with more layers of polyelectrolyte but assembled on polystyrene sulfonate colloidal particles, which dissolved in the presence of  $\text{NH}_4(\text{HCO}_3)$  during several hours.<sup>23</sup> In the case of MF the dissolution of the core is achieved by its hydrolysis to oligomers at low pH. Part of the permeating oligomers adsorb by unspecific interactions with the polyelectrolytes and influence additionally the resulting polymer film.<sup>26</sup> This has to be taken into account while discussing the influence of salt solutions on the film properties and the stability of the capsules.

## Conclusions

It was shown that PSS/PAH capsules templated on weakly polymerized MF particles are influenced by the presence of salts at moderate concentrations not higher than 1.7 M. An effect of significant size reduction with simultaneous increase of wall thickness and decrease of permeability for small fluorescent dyes was found for  $\text{KCl}$ ,  $\text{CsCl}$ ,  $\text{NaHCO}_3$ ,  $\text{NH}_4(\text{HCO}_3)$  and  $\text{Na}_2\text{CO}_3$ . The critical concentration varied from 0.2 M for  $\text{NaHCO}_3$  to 1 M for  $\text{KCl}$ ,  $\text{CsCl}$  and  $\text{NH}_4(\text{HCO}_3)$ .

The effect of alkali chlorides and sodium phosphates is rather weak and corresponds to the position of the ions in the Hoffmeister series. The behaviour of stoichiometric complexes in these solutions correlates with the weak effects of size reduction and thickness increase.

The most dramatic effects were found for  $\text{NaHCO}_3$ ,  $\text{NH}_4(\text{HCO}_3)$  and  $\text{Na}_2\text{CO}_3$  with a capsule size reduction of 20 to 25%, a wall thickness increase of 100 to 400% and strongly restricted permeability for FITC labeled dextran of low molecular weight and fluorescein. The surface charge of the capsules changed from initially positive to negative after 24 hours of incubation in each of the carbonate solutions. A partial dissolution of approx. 16% was detected for the uppermost PAH layers by fluorescent labeled PAH. This is in agreement with the dissolution kinetics of stoichiometric PSS/PAH complexes in the presence of carbonates. For the explanation of the complete charge reversal one has to take into account the strong interaction of the carbonates with the weak polyelectrolyte PAH, which was confirmed by ITC measurements. Chemical reaction and a carboxylation of the amino groups of PAH can not be excluded.

## Experimental

### Materials

The sources of chemicals were as follows: poly(styrene sulfonate, sodium salt) (PSS), MW 70000, Aldrich; poly(allylamine hydrochloride) (PAH), MW 70000, Aldrich;  $\text{LiCl}$ ,  $\text{CsCl}$ ,  $\text{NaCl}$ ,  $\text{KCl}$ ,  $\text{Na}_2\text{CO}_3$ ,  $\text{NaHCO}_3$ ,  $\text{NH}_4(\text{HCO}_3)$ ,  $\text{Na}_2\text{HPO}_4$ , and  $\text{NaH}_2\text{PO}_4$ , Merck; fluorescein and FITC-dextran, MW 4400, Sigma.

Weakly polymerised melamine formaldehyde (MF) particles ( $\text{Ø } 4.6 \pm 0.1 \mu\text{m}$ , 10% (v/v) suspension in water) were obtained from Microparticles GmbH, Berlin, Germany.

### Capsule preparation and salt treatment

Eight layers of PSS and PAH were adsorbed on MF particles applying the layer-by-layer technique. The outermost layer was PAH. The coating was performed in the presence of 0.5 M  $\text{NaCl}$ . The end concentration of both polyelectrolyte species in the solution was  $2.5 \text{ mg ml}^{-1}$  and the particle concentration was 5% (v/v). After each adsorption step the particles were centrifuged at  $1200 \times g$ , washed three times with distilled water and resuspended in 0.5 M  $\text{NaCl}$  to the initial volume of the suspension before the next polyelectrolyte solution was added. The core dissolution was carried out in 0.1 M  $\text{HCl}$  solution at a pH value between 1 and 1.5. Finally, the obtained



hollow polyelectrolyte capsules were washed several times in water until a pH value above 6 was reached and then stored in distilled water at 4 °C.

### Electrophoretic measurements

The electrophoretic mobility and the  $\zeta$  potential of the polyelectrolyte capsules were measured by means of an electrophoresis particle analyser Malvern Zetasizer 3000HS (Malvern Instruments, UK). The measurements were performed in deionized water.

### Confocal laser scanning microscopy (CLSM) and FRAP measurements

Confocal images were taken with a confocal laser scanning microscope from Leica (Germany), equipped with a 100 $\times$  oil immersion objective.

The influence of salt on the capsule size was studied both “live” under the microscope and after 24 h incubation at room temperature. The capsule size was obtained analysing sample scans at zoom 4 applying the Leica CLSM software. From each sample 30 to 50 capsules were measured.

Permeability measurements were performed with fluorescein and FITC-dextran (MW 4400) as fluorescent probes. Bleaching experiments and fluorescence recovery measurements were accomplished as described in ref. 19. Briefly, one measures the fluorescence intensity from the capsule interior following a bleaching pulse. The time dependence is given by an exponential,

$$I(t) = I(0) \cdot (1 - e^{-\frac{A}{V}Pt})$$

from which the permeability  $P$  can be derived. Here  $I(0)$  is the fluorescence intensity immediately after photo-bleaching,  $A$  is the surface area and  $V$  is the volume of a capsule interior.

### Atomic force microscopy (AFM)

AFM images have been recorded in air at room temperature using a Nanoscope III Multimode AFM (Digital Instrument Inc., Santa Barbara, CA) in contact mode. Micro-lithographed tips on silicon nitride (Si<sub>3</sub>N<sub>4</sub>) cantilevers with a force constant of 0.58 N m<sup>-1</sup> (Digital Instrument) were used. AFM images were processed by using the Nanoscope software. Samples were prepared by applying a drop of the capsule solution onto a freshly cleaved mica substrate. After allowing the capsules to settle the substrate was extensively rinsed in Millipore water and then dried under a gentle stream of nitrogen. The wall thickness was measured applying the Nanoscope software as the half of the height difference between the support and the lowest flat area point of the capsule surface profile.

### Isothermal titration calorimetry (ITC)

Titration calorimetry measurements were performed using a VP-ITC Microcalorimeter, MicroCal, MA, USA. The volume of the measuring cell was 1.442 ml. The reference cell was filled with water, the solvent in which the polyelectrolyte and the salts were dissolved. Small aliquots of salt (typically 5 or 10  $\mu$ l) were consecutively injected into the polymer solution. The

measurements were then compared to reference titrations where the salt was injected into water only. The monomer concentration of the polyelectrolyte solutions was 9.3 mM for PAH and 4.6 for PSS, respectively. The concentration of the salt solution was 50 mM. The content of the measuring cell was constantly stirred by the syringe tip at 350 rpm. All experiments were performed at 25 °C.

### Acknowledgements

We would like to thank H. Zastrow for zeta-potential measurements and A. Heilig for capsule thickness measurements. We gratefully acknowledge the German Ministry of Education and Science for financial support of the project 031201B.

### References

- 1 G. Decher, *Science*, 1997, **277**, 1232–1237.
- 2 G. Decher, B. Lehr, K. Lowack, Y. Lvov and J. Schmitt, *Biosens. Bioelectron.*, 1994, **9**, 677–684.
- 3 Y. Lvov, K. Ariga, I. Ichinose and T. Kunitake, *J. Am. Chem. Soc.*, 1995, **117**, 6117–6123.
- 4 G. B. Sukhorukov, E. Donath, H. Lichtenfeld, E. Knippel, M. Knippel and H. Möhwald, *Colloids Surf. A*, 1998, **137**, 253–266.
- 5 G. B. Sukhorukov, E. Donath, S. Davis, H. Lichtenfeld, F. Caruso, V. I. Popov and H. Möhwald, *Polym. Adv. Technol.*, 1998, **9**, 759–767.
- 6 E. Donath, G. B. Sukhorukov, F. Caruso, S. Davis and H. Möhwald, *Angew. Chem.*, 1998, **37**, 2202–2205.
- 7 B. Neu, A. Voigt, R. Mitlöhner, S. Leporatti, C. Y. Gao, E. Donath, H. Kiesewetter, H. Möhwald, H. Meiselman and H. Bäuml, *J. Microencapsulation*, 2001, **18**, 385–395.
- 8 E. Donath, S. Moya, B. Neu, G. B. Sukhorukov, R. Georgieva, A. Voigt, H. Bäuml, H. Kiesewetter and H. Möhwald, *Chem. Eur. J.*, 2002, **8**, 5481–5485.
- 9 L. Dähne and C. S. Peyratout, *Angew. Chem., Int. Ed.*, 2004, **43**, 3762–3783.
- 10 G. B. Sukhorukov, D. V. Volodkin, A. M. Günther, A. I. Petrov, D. B. Shenoy and H. Möhwald, *J. Mater. Chem.*, 2004, **14**, 2073–2081.
- 11 D. G. Shchukin, E. A. Ustinovich, G. B. Sukhorukov, H. Möhwald and D. V. Sviridov, *Adv. Mater.*, 2005, **17**, 468–472.
- 12 P. Hammond, *Adv. Mater.*, 2004, **16**, 1271–1293.
- 13 S. T. Dubas and J. B. Schlenoff, *Macromolecules*, 1999, **32**, 8153–8160.
- 14 R. Steitz, W. Jaeger and von R. Klitzing, *Langmuir*, 2001, **17**, 4471–4474.
- 15 K. Büscher, K. Graf, H. Ahrens and C. A. Helm, *Langmuir*, 2002, **18**, 3585–3591.
- 16 R. Klitzing, J. E. Wong, W. Jaeger and R. Steitz, *Curr. Opin. Colloid Interface Sci.*, 2004, **9**, 158–162.
- 17 R. Steitz, V. Leiner, R. Siebrecht and R. von Klitzing, *Colloids Surf. A*, 2000, **163**, 63–70.
- 18 S. T. Dubas and J. B. Schlenoff, *Langmuir*, 2001, **17**, 7725–7727.
- 19 G. Ibarz, L. Dahne, E. Donath and H. Möhwald, *Adv. Mater.*, 2001, **13**, 1324–1327.
- 20 R. Georgieva, S. Moya, M. Hin, R. Mitlöhner, E. Donath, H. Kiesewetter, H. Möhwald and H. Bäuml, *Biomacromolecules*, 2002, **3**, 517–524.
- 21 A. A. Antipov, G. B. Sukhorukov, S. Leporatti, I. L. Radtchenko, E. Donath and H. Möhwald, *Colloids Surf. A*, 2002, **198**, 535–541.
- 22 A. A. Antipov, G. B. Sukhorukov and H. Möhwald, *Langmuir*, 2003, **19**, 2444–2448.
- 23 J. Heuvingh, M. Zappa and A. Fery, *Langmuir*, 2005, **21**, 3165–3171.
- 24 R. Georgieva, C. Dejumat, G. B. Sukhorukov and H. Möhwald, unpublished work.
- 25 C. Y. Gao, E. Donath, S. Moya, V. Dudnik and H. Möhwald, *Eur. Phys. J. E*, 2001, **5**, 21–27.

- 
- 26 C. Gao, S. Moya, H. Lichtenfeld, A. Casoli, H. Fiedler, E. Donath and H. Möhwald, *Macromol. Mater. Eng.*, 2001, **286**, 355–361.
- 27 G. B. Sukhorukov, E. Donath, H. Lichtenfeld, E. Knippel, M. Knippel, A. Budde and H. Möhwald, *Colloids Surf. A*, 1998, **137**, 253.
- 28 S. Loporatti, A. Voigt, R. Mitlöhner, G. Sukhorukov, E. Donath and H. Möhwald, *Langmuir*, 2000, **16**, 4069.
- 29 C. Gao, S. Loporatti, E. Donath and H. Möhwald, *J. Phys. Chem.*, 2000, **104**, 7144–7149.
- 30 J. Ruths, F. Esser, G. Decher and H. Riegler, *Langmuir*, 2000, **16**, 8871–8878.
- 31 H. Dautzenberz and J. Kritz, *Langmuir*, 2003, **19**, 5204–5211.
- 32 I. Jelesarov and H. R. Bassard, *J. Mol. Recognit.*, 1999, **12**, 3–8.
- 33 R. Dimova, R. Lipowsky, Y. Mastai and M. Antonietti, *Langmuir*, 2003, **19**, 6097–6103.
- 34 C. G. Sinn, R. Dimova and M. Antonietti, *Macromolecules*, 2004, **37**, 3444–3450.